Astron. Astrophys. 353, 10–24 (2000)

ASTRONOMY AND ASTROPHYSICS

Constraining (Ω, λ) from weak lensing in clusters: the triplet statistics

L. Gautret[1], **B. Fort**[2], **and Y. Mellier**[1,2]

[1] DEMIRM, Observatoire de Paris, 61 Av. de l'Observatoire, 75014 Paris, France and URA 336 du CNRS
[2] Institut d'Astrophysique de Paris, 98 bis boulevard Arago, 75014 Paris, France

Received 22 December 1998 / Accepted 18 October 1999

Abstract. We present a new geometrical method, the *triplet statistics*, which uses weak gravitational lensing effects around clusters to constrain the cosmological parameters Ω and λ.

On each background galaxy, a cluster induces a magnification which depends on the local convergence and shear terms and on the *cosmological parameters* (Ω, λ) through the angular distance ratio D_{LS}/D_{OS}. To disentangle the effects of these three quantities, we compare the ellipticities of each triplet of galaxies located at about the same apparent position in the lens plane, but having different redshifts. The simultaneous knowledge of ellipticities and redshifts of each triplet enable to build a purely geometrical estimator (hereafter the $G(\Omega, \lambda)$-estimator) independently of the lens potential.

More precisely G has the simple form of the determinant of a 3-3 matrix built with the triplet values of D_{LS}/D_{OS} and observed ellipticities. When G is averaged on many triplets of galaxies, it provides a global function of (Ω, λ) which converges to zero for the true values of the cosmological parameters.

The calculation and the comparison of each source of statistical noise is performed. The linear form of G regarding the measured ellipticity of each galaxy implies that the different noises on G decrease as $1/\sqrt{N}$, where N is the total number of observed distorted galaxies.

The possible systematics are analyzed with a multi-screen lensing model in order to estimate the effect of perturbative potentials on galaxy triplets. Improvements are then proposed to minimize these systematics and to optimize the statistical signal to noise ratio.

Finally, simulations are performed with realistic geometry and convergence for the lensing clusters and a redshift distribution for galaxies similar to the observed ones. They lead to the encouraging result that a significant constraint on (Ω, λ) can be reached: $\lambda^{+0.3}_{-0.2}$ in the case $\Omega + \lambda = 1$ or $\Omega^{+0.3}_{-0.25}$ in the case $\lambda = 0$ (at a 1σ confidence level). These constraints would be obtained from the observations of nearly 100 clusters, using multicolor imaging in order to get photometric redshifts of triplets. This corresponds to about 20 nights of VLT observations. The method looks even more promising with the NGST, in particular if it was used jointly with the supernovae search which provides orthogonal constraints.

Send offprint requests to: Yannick Mellier (mellier@iap.fr)

Key words: galaxies: clusters: general – cosmology: observations – cosmology: dark matter – cosmology: gravitational lensing

1. Introduction

Determination of the cosmological parameters of the standard cosmological models is one of the great challenges for the next ten years. Though these are the main objectives of the MAP and Planck Surveyor satellites, considerable efforts are devoted to the measurements of the (Ω, λ)[1] parameters prior to the launch of these surveyors. In this respect, the supernovae search (see the Supernova Cosmological Project, Perlmutter et al. 1998) or gravitational lensing surveys (for a review see Mellier 1998) offer interesting perspectives. If they are used together, the analysis of the joint constraints can increase significantly the reliability of the results and produce precise (Ω,λ) confidence maps if the degeneracy regarding the determination of parameters (Ω, λ) of each method is almost orthogonal. This is for instance the case for the supernovae experiments and the lensing statistics (Efstathiou et al. 1999, Helbig 1999), the weak lensing analysis induced by large-scale structures (Van Waerbeke et al. 1999) or the new method presented hereinafter.

The limitations of any of these methods are the understanding of the systematic biases and the control of the large number of free parameters attached to each of them. Due to the difficulties to handle these issues, it is important to diversify the observational tests which can measure (Ω, λ). In this regard, any new method that controls properly its own systematics and that decreases the number of sensitive parameters needs careful attention. Those using gravitational lensing effects are based on the sensitivity of angular distances to cosmological parameters.

Applications of this property to lensing clusters have been proposed by Breimer & Sanders (1992) and Link & Pierce (1998). They suggest to use giant arcs having different redshifts to probe directly the curvature of the Universe from their different angular position. This method can provide the cosmological parameters in the simplest way, provided that the modeling of

[1] Ω is the matter density to critical density ratio. λ is the ratio $\Lambda/3H_0^2$, where H_o is the Hubble constant.

the lens is perfectly constrained. Furthermore, it requires the spectroscopic redshifts of at least two different arcs in the same clusters, which is not an easy task. As such, it will apply to very few clusters.

Fort, Mellier & Dantel-Fort (1996) focused on a statistical approach which explores the magnification bias coupled with the redshift distribution of the sources. They used the shape and the extension of the depletion curves produced by the magnification of the galaxies to constrain the cosmological parameters and the redshift of the sources simultaneously. The intrinsic degeneracy can be broken if the redshift of at least one giant arc is known and if the number density of high-redshift background galaxies is large enough. However, in practice, reliable results need the investigation of a significant number of lensing arc-clusters in order to improve the statistics, to minimize the systematics (like multiple lens planes) and to explore the sensitivity to the lens modeling.

The key issue on the Fort et al. approach is the coupling between the cosmological parameters, the redshift of the sources and the lens modeling. An interesting attempt to disentangle these three quantities has been proposed by Lombardi & Bertin (1998). It uses a method which applies in rich clusters of galaxies, inside the region where the weak-lensing approximation is valid. They use the knowledge of the photometric redshifts for a joint iterative reconstruction of the mass of the cluster and the cosmology. Their iteration method assumes that the mass of the deflecting cluster is known (or equivalently they assume that the mass-sheet degeneracy inherent to the mass reconstruction is broken). This assumption is a critical point, because it means that a perfect correction of the biases on the (Ω, λ) determination due to the systematic errors in the mass reconstruction (see Sect. 3.1) can be achieved, which is still not presently the case (see Mellier 1998 for a comprehensive review). More generally, the tests of curvature from gravitational lensing effect of individual lenses have uncertainties which are mainly dominated by the errors on the reconstruction of the mass distribution of the lens.

The alternative triplet statistics proposed in this paper can solve this problem because it is based on a (Ω,λ)-estimator independent of the lens potential. Basically, it consists in comparing the shear amplitude of 3 galaxies having different redshifts (which can be obtained from multi-color photometry) and which are at about the same apparent position on the sky, so that their photons experience the cluster gravitational potential at the same position. When the galaxies are close enough, their ellipticity only depends on three unknown parameters, the local convergence and shear (related to the second order derivatives of the projected potential of the cluster) and the cosmological parameters (Ω, λ), through the angular distance ratio D_{LS}/D_{OS}. The use of a triplet of neighboring galaxies enables to break this degeneracy and provides a local geometrical operator which only depends on (Ω, λ). We have defined a local linear operator regarding the observed ellipticities, and we average it on all set of close-triplets detected in many lens planes. It can be shown that the noise of this estimator (coming mainly from the intrinsic source ellipticities) decreases as the inverse of the square root of the number of triplets, which means that with a large number of lensing clusters one can estimate (Ω, λ) with a reasonable accuracy. This technique and its efficiency are discussed in the following sections.

Sect. 2 summarizes the lensing equations and the basic lensing quantities relevant for the paper. In Sect. 3, we build the geometrical estimator G which uses triplets of distorted galaxies. The principle and the detailed analysis of our method are also discussed. The signal to noise ratio is then derived as well as the probability distribution of the cosmological parameters (Ω,λ). Sect. 4 gives an evaluation of the amplitude of several systematic biases coming from possible perturbing lenses distributed along the line of sight of triplets (galaxies or larger structures). Though it is beyond the scope of this paper to deal with the systematics into great details, preliminary solutions to handle these systematic biases and ideas of optimizing the triplet statistics are developed in Sect. 5. The method is tested on simulations in Sect. 6. Finally, we discuss the results and suggest some observational strategies in Sect. 7.

2. The weak lensing equations

The lensing properties are determined by the dimensionless convergence κ (the strength of the lens) and the shear[2] $\boldsymbol{\gamma}$ (the distortion induced by the lens), which both depend on the second order derivatives of the two-dimensional projected deflecting potential. The lensing effect of a cluster on background galaxies can be expressed as an amplification matrix defined in each angular position around the cluster as (Schneider et al. 1992)

$$A^{-1} \;=\; \begin{pmatrix} 1-\kappa-\gamma_1 & -\gamma_2 \\ -\gamma_2 & 1-\kappa+\gamma_1 \end{pmatrix} , \tag{1}$$

where

$$\boldsymbol{\gamma} = \gamma_1 + i\gamma_2. \tag{2}$$

κ is a dimensionless surface mass density Σ:

$$\kappa = \Sigma/\Sigma_{crit} \text{ with } \Sigma_{crit} = \frac{c^2}{4\pi G D_{OL}} \frac{D_{OS}}{D_{LS}} , \tag{3}$$

where D_{OS}, D_{OL} and D_{LS} are the angular diameter distances from the observer to the source, from the observer to the lens and from the lens to the source respectively. For the weak lensing regime the gravitational distortion produced by a lensing cluster can be modeled by a transformation in the ellipticity of the galaxies from the source plane (ϵ_S) to the image plane (ϵ) (see Appendix A):

$$\boldsymbol{\epsilon} = (1-g^2)\boldsymbol{\epsilon}_S + \boldsymbol{g} = \bar{\boldsymbol{\epsilon}}_S + \boldsymbol{g} \quad \text{with} \quad \boldsymbol{g} = \frac{\boldsymbol{\gamma}}{1-\kappa}. \tag{4}$$

$\boldsymbol{\epsilon}$ is the complex observed ellipticity, $\boldsymbol{g}$ is the complex reduced shear and $\bar{\boldsymbol{\epsilon}}_S$ is what we will call the complex corrected source

[2] In the following mathematical notations with bold letters refer to complex numbers while usual letters are used for scalars or for the norm of the associated complex numbers. The upper * index behind a complex number indicates its conjugated element.

ellipticity. The ellipticity parameter of the galaxies in the source plane and the image plane is defined by:

$$\boldsymbol{\epsilon} = \epsilon\, e^{2i\theta} \text{ with } \epsilon = \frac{1-r}{1+r}; \tag{5}$$

r is the axis ratio of the image isophotes and θ is the orientation of the main axis.

The convergence and the shear both depend on the source redshift through an absolute lensing factor ω_a appearing in Eq. (3):

$$\omega_a(z) = \frac{D_{LS}}{D_{OS}}\ . \tag{6}$$

Adopting the notation of Seitz & Schneider (1997) who relate the lensing parameters to the value they would have at infinite redshift, κ and γ now write:

$$\kappa\ =\ \omega(z)\kappa_\infty\ ;\ \boldsymbol{\gamma} = \omega(z)\boldsymbol{\gamma}_\infty\ ,\ \text{where} \tag{7}$$

$$\omega(z)\ =\ \frac{\omega_a(z)}{\omega_a(\infty)}\ . \tag{8}$$

Hereafter, $\omega(z)$ will be named the lensing factor. This is the term which contains the cosmological dependency.

3. The triplet statistics

The behavior of $\omega(z)$ with Ω in the case $\Omega + \lambda = 1$ (flat geometry) and in the case $\lambda = 0$, is given on Fig. 1. All curves range from 0 (for a source redshift equal to the cluster redshift) to 1 (for an infinite source redshift). Their main difference is a small change in their convexity. The method we propose is a test on the convexity of $\omega(z)$ curves, that is why the use of numerous triplets of sources at different redshifts may disentangle cosmological models, i.e. provide a constraint on the cosmological parameters.

The key point of the method results from Eqs. (7),(8) and (9) which imply that it is possible to separate the effect of the mass distribution to those from the cosmology. Only κ_∞ and γ_∞ depend on the modeling, while only $\omega(z)$ depends on the cosmological model and the redshifts. We have then constructed an operator which depends theoretically on (Ω, λ) and can be computed directly from the observed ellipticities of background galaxies as well as from their redshift (the use of photometric redshifts allows to get a large number of triplets per cluster). Its main property is to be equal to zero when the cosmological parameters are the actual ones. We proceed in two steps: first, we build the operator (G_{ijk}) from triplets of close sources, and second we average it on many triplets of sources to obtain the final geometrical operator G.

3.1. Construction of G_{ijk}

For a background galaxy at redshift z_i, Eq. (4) rewrites

$$\boldsymbol{\epsilon}_i\ =\ \bar{\boldsymbol{\epsilon}}_{S,i} + \boldsymbol{g}_i^o \text{ with} \tag{9}$$

$$\boldsymbol{g}_i^o\ =\ \frac{\omega_i^o \boldsymbol{\gamma}_\infty}{1 - \omega_i^o \kappa_\infty}, \tag{10}$$

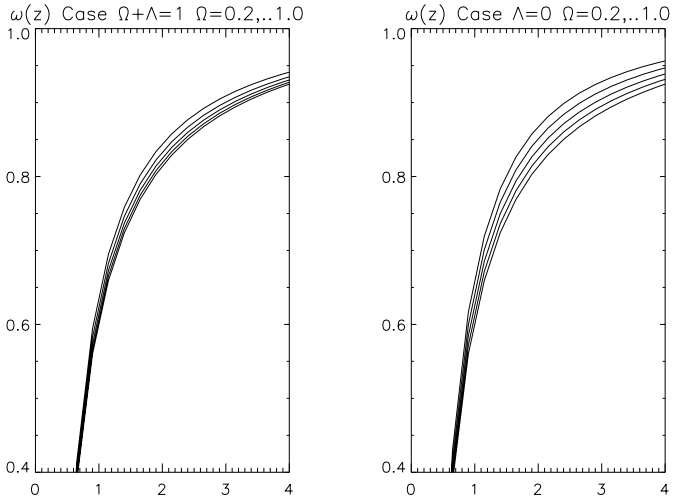

Fig. 1. ω versus redshift in the cases $\Omega + \lambda = 1$ and $\lambda = 0$, for a cluster lying at a redshift 0.4. Different curves correspond to $\Omega = 0.2$ (top curve), $0.4, 0.6, 0.8$ and 1.0 (bottom curve). All curves start from 0 (at redshift 0.4) and converge to 1.0 when the redshift becomes infinite. The triplet statistics probes their relative convexity.

where the lower index (i) refers to the redshift z_i and the upper index $(^o)$ refers to the actual values of the cosmological parameters: Ω_o,λ_o. The second term in Eq. (10), $\boldsymbol{g}_i^o$, represents the part of the image ellipticity that depends on the cosmology.

Let us now consider a triplet of background neighboring galaxies in the image plane lying at redshifts z_i, z_j and z_k. The number density of triplets depends on the deepness of the observations. For instance, up to $R = 26$ mag., we expect a mean density of 50 sources arcmin^{-2}, that is about 4 sources inside a circle of radius 10 arcseconds. In the following, we thus consider that each galaxy of the triplet is distorted by the same local potential i.e. κ_∞ and $\boldsymbol{\gamma}_\infty$ are the same for the three galaxies. The bias induced by this approximation will be discussed in Sect. 3.4. The triplet of galaxies gives a triplet of Eqs. (11) respectively indexed by i, j and k from which we can derive a final equation independent both on κ_∞ and $\boldsymbol{\gamma}_\infty$. This equation writes simply as the zero of a 3-3 determinant:

$$\begin{vmatrix} 1 & \omega_i^o & \omega_i^o g_j^o g_k^o \\ 1 & \omega_j^o & \omega_j^o g_k^o g_i^o \\ 1 & \omega_k^o & \omega_k^o g_i^o g_j^o \end{vmatrix} = 0\ . \tag{11}$$

The first term of this equation can now be formally generalized to a complex operator G_{ijk} of (Ω, λ) built from the complex measured ellipticities of the three galaxies:

$$G_{ijk}(\Omega, \lambda) = \begin{vmatrix} 1 & \omega_i & \omega_i \boldsymbol{\epsilon}_j \boldsymbol{\epsilon}_k^* \\ 1 & \omega_j & \omega_j \boldsymbol{\epsilon}_k \boldsymbol{\epsilon}_i^* \\ 1 & \omega_k & \omega_k \boldsymbol{\epsilon}_i \boldsymbol{\epsilon}_j^* \end{vmatrix}\ . \tag{12}$$

The dependency in (Ω, λ) is contained in each term $\omega_s(\Omega, \lambda)$ ($s = i$, j or k) defined by Eq. (9) for $z = z_s$. G_{ijk} is more explicitly the sum of two (Ω, λ) functions: G_{ijk}^{main} which is equal to zero for the actual values of the cosmological parameters, and a complex noise N_{ijk} (that will be discussed in 3.4):

$$G_{ijk} = G_{ijk}^{main} + N_{ijk}\ , \tag{13}$$

where

$$G_{ijk}^{main} = \begin{vmatrix} 1 & \omega_i & \omega_i g_j^o g_k^o \\ 1 & \omega_j & \omega_j g_k^o g_i^o \\ 1 & \omega_k & \omega_k g_i^o g_j^o \end{vmatrix} . \quad (14)$$

At this point it is important to stress that the κ_∞ contribution cannot be neglected (see Eq. (11)). Indeed, if we consider for instance a 10% variation of the cosmological parameters (along the gradient of $\omega(\Omega, \lambda)$), the resulting relative variation of the term $\omega\gamma$ is about 1% which is about ten times smaller than the relative variation due to the $1 - \omega\kappa$ term, in Eq. (11). That is why both contributions from the local convergence (κ_∞) and the local shear (γ_∞) of the cluster potential must be taken in account.

Lombardi & Bertin (1998) proposed to reconstruct jointly the shear, the convergence and (Ω, λ) in the weak lensing area, with an iterative procedure based on the Eq. (11). Their method seems to converge rapidly with a small number of clusters but it seems that for their simulations they implicitly assume that the mass of the cluster is known. However, one can see that Eq. (11) is invariant when replacing γ_∞ by $\alpha\gamma_\infty$ and $1 - \omega\kappa_\infty$ by $1 - \alpha\omega\kappa_\infty$ (α is a constant). This expresses the mass-sheet degeneracy problem which implies that the total mass of the lensing cluster is uncertain. Numerous suggestions have been proposed in order to solve this issue (Seitz & Schneider, 1997). However, even if it is possible to break the degeneracy, other systematic errors which are still not well understood can produce biases (Mellier 1998). As an example, a 20% systematic bias on the determination of the total mass of the cluster (or equivalently a 20% systematic on the mean value of κ_∞) is equivalent to a systematic bias larger than 0.2 on the value of the cosmological parameters (when compared to the 1% contribution from the lensing factor mentioned above). Therefore, the knowledge of the lens potential is a critical strong assumption.

In the triplet statistics, it is possible to constrain the cosmological parameters regardless the potential of the lens. No assumption on the mass distribution is made in order to relate the values of the local shear to the local convergence. Hence they are considered as independent parameters. In order to construct a G operator which only depends on (Ω, λ), we then need three local equations relating κ_∞, γ_∞ and (Ω, λ) to cancel the potential dependency. This is achieved with the measured ellipticity Eqs. (10) applied to triplets of close galaxies at different redshifts. Furthermore, if we want the G operator to be linear with respect to the ellipticities provided by the observations, its form is unique and must have the formal expression given in Eq. (13). In summary, the use of triplets of galaxies through the operator G is the simplest way to build a pure geometrical operator which drops both the κ_∞ and γ_∞ dependencies and keeps linear regarding to the ellipticities.

The statistical noise N_{ijk} will be more explicitly calculated in Sect. 3.4 and Annex C. At this stage, it is just worth noting that the probability distribution of this noise (real and imaginary parts) regarding the different triplets of galaxies is a random law centered on zero. This results from linear construction of G which makes the sources of noise (mainly the intrinsic source ellipticity) be randomly distributed around 0.

3.2. Construction of G

Since the G_{ijk} are defined from arclets having different redshifts, the average over many triplets could be zero because of the random redshift distribution of the galaxies inside each triplet. In order to avoid this, we first arrange the redshift of galaxies inside triplets in ascending order: $z_i < z_j < z_k$. We can then derive G from these ordered triplets ijk:

$$G(\Omega, \lambda) = \langle G_{ijk} \rangle , \quad (15)$$

where the brackets denote the average over all triplets. According to Eq. (14), G is also composed of two terms: the first one G^{main} which has the same properties as G_{ijk}^{main}, and a Gaussian noise GN which decreases as $1/\sqrt{N}$,

$$R_e(G)(\Omega, \lambda) = G^{main}(\Omega, \lambda) + Re(GN) , \quad (16)$$

where

$$G^{main} = \left\langle \begin{vmatrix} 1 & \omega_i & \omega_i g_j^o g_k^o \\ 1 & \omega_j & \omega_j g_k^o g_i^o \\ 1 & \omega_k & \omega_k g_{ji}^o g_j^o \end{vmatrix} \right\rangle \approx \quad (17)$$

$$\left\langle \begin{vmatrix} 1 & \omega_i & \omega_i/\omega_i^o \\ 1 & \omega_j & \omega_j/\omega_j^o \\ 1 & \omega_k & \omega_k/\omega_k^o \end{vmatrix} \omega_i^o \omega_j^o \omega_k^o \gamma_\infty^2 \right\rangle ,$$

and

$$R_e(GN) \propto 1/\sqrt{N} , \quad (18)$$

where R_e denotes the real part of the complex quantities. We consider the real part of G ($Re(G)$) because as N, the noise GN is complex.

By construction G^{main} is equal to zero at the position (Ω_o, λ_o). We thus can write the following equation (affected by the presence of the Gaussian noise) which sums up the method: (Ω_o, λ_o) is a solution of

$$G(\Omega, \lambda) \equiv 0. \quad (19)$$

In order to see if the triplet statistics can be effective from the observational point of view three questions have to be addressed:

1. how is the G-operator degenerated in (Ω, λ)?
2. how many clusters are necessary to cancel the noise contribution with respect to the cosmological information contained in G^{main}?
3. what are the main systematic biases?

3.3. The main cosmological term: $G^{main}(\Omega, \lambda)$

Let us now consider the behavior of the main cosmological quantity G^{main}. Although it obviously depends on the mass of the cluster through the κ_∞ and γ_∞ terms, we can qualitatively separate this operator in two terms, one sensitive to the mass distribution of the lens and another one sensitive to the redshift

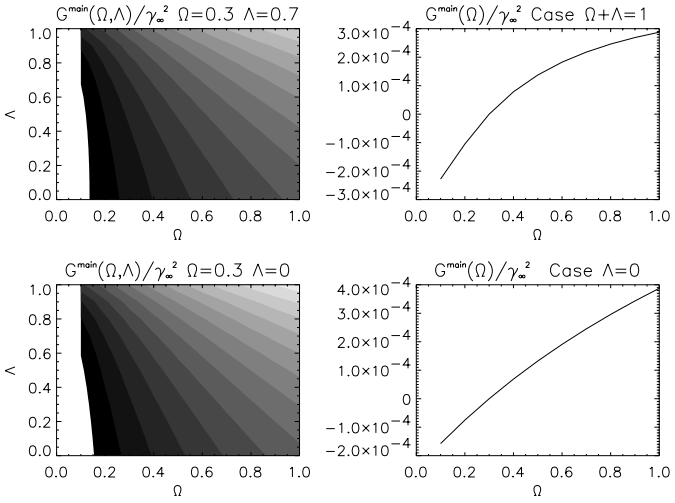

Fig. 2. Contours of $G^{main}(\Omega,\lambda)/\left\langle\gamma_\infty^2\right\rangle$ in the cases $(\Omega,\lambda) = (0.3, 0.7)$ (top panel) and $(0.3, 0)$ (bottom panel). $\left\langle\gamma_\infty^2\right\rangle$ is the square of γ_∞ averaged over the weak lensing area. $\left\langle\gamma_\infty^2\right\rangle$ is the square of γ_∞ averaged on the weak lensing area. The right part of the figure gives the restriction of G^{main} to the particular domains $\Omega + \lambda = 1$ (top) and $\lambda = 0$ (bottom).

distribution of the sources. From Eq. (11), we see that if we neglect the small contribution from the κ_∞ term, g_s^o ($s = i, j$ or k) is proportional to the norm of the local shear γ_∞. In order to get a qualitative estimate of G^{main} independently of the total mass of the clusters, let us assume for a short while that the density distribution of galaxies in the image plane is independent of their redshift distribution, so that we can separate the average over redshifts to the average over the projected positions galaxies inside triplets (this approximation means that additional clustering effects along the line of sight are neglected, which is a rough approximation, but becomes justified when the number of clusters is high). We can then average separately the γ_∞^2 (coming from terms like $g_j^o g_k^o$ in (18)) on all the triplets.

Fig. 2 gives the contours of $G^{main}/\left\langle\gamma_\infty^2\right\rangle$ in the (Ω, λ) plan, for the redshift distribution (38), as taken in the simulations (see Sect. 6). From this graph we see that the method is degenerated in (Ω, λ). The degeneracy is parallel to the G-contours. To break this degeneracy one has either to make a theoretical assumption (for example $\Omega + \lambda = 1$) or to add other constraints, like those from the high-redshift supernovae experiments (Perlmutter et al. 1998) which have contours orthogonal to our estimator. From Fig. 2 we also get quantitatively the variations of G. It shows that, for an accuracy of about 10% on the cosmological parameters (along the gradient of G), we obtain a precision of about $10^{-4}\left\langle\gamma_\infty^2\right\rangle$ on G. This rate of variation has to be compared with the noise on G.

3.4. Noise on G

As it is shown in Annex C, the complex noise is produced by four sources:

1. the noise from the corrected source ellipticities $\bar{\epsilon}_{S,i,j,k}$,
2. the errors propagation on the measured ellipticities $\Delta\epsilon_{i,j,k}$ (it behaves similarly as the previous ones),
3. the fact that the three sources do not have exactly the same γ_∞ and we thus have to consider $\Delta\gamma_{\infty,i,j,k}$ (in other words, each source, though close to each other, do not exactly cross the potential at the same position)
4. the photometric redshifts are not the exact redshifts and lead to shifts $\Delta\omega_{i,j,k}$ on the lensing factors.

Due to the linearity of the 3-3 determinant (see Annex C) and of the averaging on all the triplets, the final noise is linear relatively to each individual term. Therefore, it is centered on zero and decreases as the inverse of the square root of the number of sources. The relative weight of each source of noise can be qualitatively described from the simulations we performed in Sect. 6. The value of their approximate variance (respectively noticed $GN_{\bar{\epsilon}_S}, GN_{\Delta\epsilon}, GN_{\Delta\omega}$ and $GN_{\Delta\gamma_\infty}$ for the four sources of noise presented above), is roughly given by the following empirical behavior:

$$GN_{\bar{\epsilon}_S} \approx 0.08\frac{\left\langle\gamma_\infty^2\right\rangle}{\sqrt{N}}\,, \tag{20}$$

$$GN_{\Delta\epsilon} \approx 0.02\frac{\left\langle\gamma_\infty^2\right\rangle}{\sqrt{N}}\,, \tag{21}$$

$$GN_{\Delta\omega} \approx 0.04\frac{\left\langle\gamma_\infty^2\right\rangle}{\sqrt{N}}\,, \tag{22}$$

$$GN_{\Delta\gamma_\infty} \approx 0.02\frac{\left\langle\gamma_\infty^2\right\rangle}{\sqrt{N}}\,. \tag{23}$$

Hence, the intrinsic ellipticity distribution of the sources dominates the noise budget of our estimator.

3.5. Resulting signal to noise ratio

Let us establish the relation between the signal to noise ratio of the estimator and the number of background galaxies (or equivalently the number of clusters in the sample). If we define the signal as a variation of G^{main} along its gradient and σ_{GN} as the variance of the statistical noise (see Sect. 3.4), the signal to noise ratio can thus be written as:

$$S/N = \frac{\Delta G^{main}}{\sigma_{GN}} = \frac{\Delta_{\Omega,\lambda}\left|\left|\nabla G^{main}_{|\Omega_o,\lambda_o}\right|\right|}{\sigma_{GN}}\,, \tag{24}$$

where $||...||$ denotes the norm of a vector. $\Delta_{\Omega,\lambda}$ is the accuracy on the cosmological parameters. Fig. 3 plots the variation of $\Delta_{\Omega,\lambda}$ as a function of the number of clusters (with an observed number density of background galaxies equal to 50 per square-arcminute) for a 1σ confidence level. This plot shows that an accuracy of about 0.3 can be reached (at a 1σ level) with 100 clusters and 1000 background galaxies per cluster, or similarly an accuracy of 0.1 (1σ) with about 1000 clusters.

It shows that with a good seeing one could in principle test the existence of a cosmological constant and estimate its value from a deep survey of about 100 clusters with the VLT. Since the triplet statistic uses lensed galaxies with shear ranging between

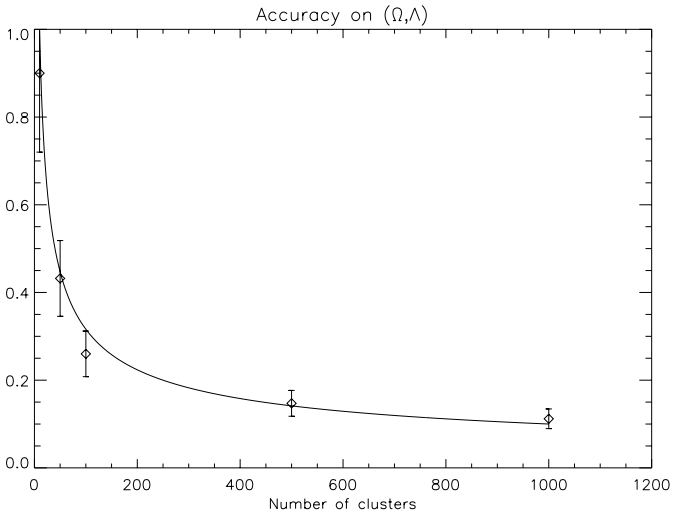

Fig. 3. Accuracy on the cosmological parameters versus the number of clusters (with 1000 galaxies per cluster) at a 1σ confidence level. The plain line extrapolates the results obtained from simulations with an inverse square root function. Error bars account for the number of simulations. We can read that a 0.3 accuracy (at 1σ) can be achieved with the observations of 100 clusters and a 0.1 accuracy (at 1σ) can be achieved with the observations of 1000 clusters. With the NGST, the number density of lensed sources will increase by a factor of 10, so the much larger number of triplets will improve considerably the statistics.

2% to 20%, the typical field of view needed range between $1'$ to $10'$. Therefore, the triplet statistics is a good program for FORS on the VLT. Far better it should be possible to measure the curvature of the Universe with a good accuracy from NGST deep observations, which will multiply by a factor of 10 with respect to the VLT the number density of background. More exactly it constrains (Ω, λ) along the degeneracy of G. As shown on Fig. 2, the degeneracy of G is approximately parallel to $\lambda + \Omega$. This direction slightly differs with different source redshift distributions). These prospects of course require that the systematics are previously corrected. These results can be refined by the introduction of a probability distribution.

3.6. The (Ω, λ) probability distribution

Thanks to the probability distribution of the noise $(p_{noise}(R_e(GN)))$ we can derive a probability distribution $p(\Omega, \lambda)$ for the cosmological parameters, using a maximum likelihood:

$$p_{\Omega,\lambda}(\Omega, \lambda) \equiv p_{noise}(R_e G(\Omega, \lambda)) \ , \tag{25}$$

which has just to be normalized on the considered domain of (Ω, λ), (for example $\Omega + \lambda = 1$).

The operator $G(\Omega, \lambda)$ is directly derived from the observational data.

On the other hand, the function p_{noise} is obtained from simulations applied on the data in the following way. Once the function $G(\Omega, \lambda)$ is obtained from the observation of ($\boldsymbol{\epsilon}$, z), it is possible to add noise to the data by adding random ellipticities ($\boldsymbol{\epsilon}_S$) and random errors Δz to the redshifts z. The probability distribution of the noise $R_e(GN)$ induced on G gives the function p_{noise}.

4. Analysis of systematics

In this section we give a preliminary discussion of the systematics which could potentially reduce significantly the efficiency of the triplet statistics. Though we give estimations of their amplitude, it is worth noting that a reliable quantitative estimate of their impact on the triplet statistics will demand additional work (mainly simulations and calculations taking in account the perturbation coming from large-scale structures).

Two main systematics have been identified:

1. a systematic bias on G produced by the non-symmetry of the term $\Delta\omega$. It can be easily corrected (see 4.1),
2. a contamination produced by the existence of background structures which play the role of perturbing lenses. They can be the background galaxies themselves (which induce galaxy-galaxy lensing) or any condensation of mass (clusters or large-scale structures) located on the line of sight of the lensing cluster. In the following sections (Sects. 4.2 and 4.3), we focus on two extreme cases: the systematic produced by the galaxies of each triplet themselves, and those generated by large-scale structures. This study will be performed using multi-lensing models (see Kovner 1987). Appendix B gives the calculation of the measured ellipticities in a multi-lensing model.

4.1. Non symmetry of the term $\Delta\omega$

The method supposes that we know the (photometric) redshifts of background galaxies as well as the probability distribution $p_{\Delta z}(\Delta z)$ of the error between the photometric redshift and the true one. Even if $p_{\Delta z}(\Delta z)$ is symmetric and centered on zero, which is not necessarily the case, the probability distribution of the resulting shift on ω, $p_{\Delta\omega}(\Delta\omega)$ may be non symmetric and the mean value of $\Delta\omega$ may be different from zero, introducing a systematic in Eq. (23). Fortunately, this effect is easy to correct. Since the redshift distribution $n(z)$ is known the systematic can be exactly balanced by replacing in the definition of G_{ijk} ω by $\omega - \overline{\Delta\omega}$, where

$$\overline{\Delta\omega}(z) = \int \omega(z + \Delta z) n(z + \Delta z) p_{\Delta z}(\Delta z) d\Delta z \ . \tag{26}$$

4.2. Potential perturbation due to galaxy-galaxy lensing

Since we consider triplets of galaxies having different redshifts but which are close together in the image plane (less than 20 arcseconds), the most distant can potentially be distorted by the lensing effect of the others. In particular, in each triplet (i, j, k) (ordered with increasing redshifts) the galaxy i is a perturbation of the potential for the sources j and k as well as the galaxy j for the source k. It is worth noting that i is not the only perturbing lens for the source j, and i and j are not the only one for the source k. For instance, each galaxy may be itself part of a group

of galaxies which produces its own additional lensing effect. Nevertheless, in order to get a rough estimate of the amplitude of this kind of systematics, we will assume to first approximation that the galaxy-galaxy lensing produced within each triplet, is the dominant contribution.

The galaxy-galaxy lensing increases as the apparent angular separation between the galaxy-lens and the galaxy-source decreases. It also depends on their relative redshifts: that is why it induces a systematic bias on the construction of G. In Appendix B we compute the amplitude of the corrections on the measured ellipticities, once several lenses along the line of sight are taken into account. From Eqs. (62), (63) and (66) of Appendix B, one can see that these perturbations produce two kinds of effects:

1. a pure additive term, g^P. It can be seen as the linear contribution from the shear, as if the shears of each lenses were simply added to each other without coupling considerations,
2. a multiplicative term of the form $\left(1-(1-c)\,\kappa^P\right)^{-1}$ which modifies the main cosmological term g. It accounts for couplings between the main and additional lenses.

4.2.1. The additive linear term

Since the three galaxies of each triplet are randomly distributed and uncorrelated, this term induces a noise rather than a systematic bias. It decreases as $1/\sqrt{3N}$, like the noise $GN_{\Delta\gamma_\infty}$ for instance. Furthermore, the shear induced by a galaxy-lens can be controlled by removing the few triplets having too small apparent angular separation between the sources. This is typically lower then a few arcsecond for typical Einstein radius of galaxies. This procedure lowers the induced shear to less than 2%. Therefore the amplitude of this additive term can be bounded to less than 10% of the effect coming from the principal statistical noise $GN_{\epsilon_{S,i}}$, and thus can be neglected.

4.2.2. The multiplicative coupling term

The effect of coupling between two lenses depends on their redshifts through the angular distances ratio. Hence this term can really induce a systematic bias on G. To calculate it we have to think about the meaning of the additional convergence, κ^P, used in the multi-lens screen approach of annex B. Let this convergence produced by the galaxy-lens i on the the source j be noted $\kappa^{i,j}$ and the convergences produced by the galaxy-lenses i and j on the source k be noted $\kappa^{i,k}$ and $\kappa^{j,k}$ respectively. In order to model this systematic bias we first re-scale the convergence by associating to each source of a triplet an absolute convergence $\tilde{\kappa}^{gal}$ independent of the redshifts z_i, z_j and z_k. Obviously $\tilde{\kappa}^{gal}$ should depend on the angular separation between the galaxy-source and the galaxy lens. Here, we consider a mean value for this convergence, calculated from the mean angular separation between galaxies in each triplet, *i.e.* the radius of the circles in which we search for triplets (for the definition of this circle, see Sect. 5.2):

$$\kappa^{i,j} = \frac{D_{Oi}}{D_{OL}}\frac{D_{ij}}{D_{Oj}}\tilde{\kappa}^{gal} \tag{27}$$

$$\kappa^{i,k} = \frac{D_{Oi}}{D_{OL}}\frac{D_{ik}}{D_{Ok}}\tilde{\kappa}^{gal} \tag{28}$$

$$\kappa^{j,k} = \frac{D_{Oj}}{D_{OL}}\frac{D_{jk}}{D_{Ok}}\tilde{\kappa}^{gal}. \tag{29}$$

The shift due to the perturbation by galaxy-galaxy effects, $\Delta^{GGL}_{\Omega,\lambda}$ (along the gradient of G), on the cosmological parameters is then:

$$\frac{\left\langle \left| \begin{array}{lll} 1 & \omega_i & 0 \\ 1 & \omega_j & \frac{D_{ij}}{D_{OL}}\left(\frac{D_{Oi}}{D_{Oj}}-\frac{D_{Li}}{D_{Lj}}\right) \\ 1 & \omega_k & \frac{D_{ik}}{D_{OL}}\left(\frac{D_{Oi}}{D_{Ok}}-\frac{D_{Li}}{D_{Lk}}\right)+\frac{D_{jk}}{D_{OL}}\left(\frac{D_{Oj}}{D_{Ok}}-\frac{D_{Lj}}{D_{Lk}}\right) \end{array} \right| \right\rangle}{\left\| \nabla_{\Omega_0,\lambda_0} \left\langle \left| \begin{array}{lll} 1 & \omega_i & \omega_i/\omega_i^o \\ 1 & \omega_j & \omega_j/\omega_j^o \\ 1 & \omega_k & \omega_k/\omega_k^o \end{array} \right| \right\rangle \right\|}\tilde{\kappa}^{gal} \tag{30}$$

where the brackets $\langle ... \rangle$ denote the average over all the ordered triplets.

Using the redshift distribution (38) and considering the mean value of the convergence created by a galaxy as about 2% (see Sect. 5.2), one gets: $\Delta^{GGL}_{\Omega,\lambda} = 10.2\tilde{\kappa}^{gal} \approx 0.2$.

This is only an indicative value. More precised estimations need a better knowledge of the mass and size distributions of galaxy halos than what we have at present. In the future, we expect that the galaxy-galaxy lensing analysis will benefit from on going wide field surveys in order to provide much better constraints on these halos (see Schneider & Rix 1996). Nevertheless, we are in principle able to account for the effect of the potential of each background galaxy, so that this systematic can be calculated and corrected. If the knowledge of the mean potential of galaxies could reach a $\approx 20\%$ accuracy, the remaining systematic would then be about $\Delta^{GGL}_{\Omega,\lambda} \approx 0.04/\sqrt{Nclust}$.

This correction does not take in account the possibility that a fraction of the galaxies are embedded in compact groups which could enhance the contamination. To solve this issue, one can use the photometric redshifts of the galaxies in order to discriminate compact groups of galaxies and to remove the corresponding triplets from the sample. Eventually, if the galaxy-galaxy lensing studies made significant progresses in the future, one could in principle calculate $\Delta^{GGL}_{\Omega,\lambda}$ with a reasonable accuracy and remove its contribution to the shear signal produced by the cluster.

In conclusion this effect is non-negligible but can be accurately estimated and corrected, thanks to the coupling of the triplet statistics with galaxy-galaxy lensing analysis on blank fields.

4.3. Potential perturbation due to background lensing structures

Before considering the perturbation produced by background structures along the line of sight, let us calculate the perturbation due to a single lens plane (containing an over dense region like a cluster or even an under dense region). Since this second lens may be located anywhere in redshift, it differently affects the measured ellipticities of the sources (i, j, k) in each triplet

Table 1. The systematic biases on the determination of (Ω, λ). $\Delta^{GGL}_{\Omega,\lambda}$ is due to galaxy-galaxy lensing effects. $\Delta^{LBS}_{\Omega,\lambda}$ is due to the linear effect of the distortion induced by background structures. $\Delta^{CBS}_{\Omega,\lambda}$ comes from the coupling of these background structures with the main lens.The corrections of $\Delta^{GGL}_{\Omega,\lambda}$ and $\Delta^{LBS}_{\Omega,\lambda}$ require to adjust the method with a modeling of the potential of galaxies and large scale structures. Such modeling compared with ray tracing simulations will be performed in paper II. $\Delta^{CBS}_{\Omega,\lambda}$ can not be corrected because of its random behavior.

$\Delta^{GGL}_{\Omega,\lambda}$	≈ 0.2	corrected to $\approx 0.04/\sqrt{N_{clust}}$
$\Delta^{LBS}_{\Omega,\lambda}$	≈ 0.03	corrected
$\Delta^{CBS}_{\Omega,\lambda}$	$\approx 0.4/\sqrt{N_{clust}}$	not corrected

and therefore it can induce a systematic on the value of G. By using again the calculations done in annex B (see Eq. (66)), this systematic can be split in two parts, an additive term (corresponding to the linear contribution of the perturbative lens) and a multiplicative term (corresponding to the coupling between the main and the perturbative lenses).

4.3.1. The additive linear term

Like in the previous section, we assign an absolute convergence and an absolute shear $\delta\tilde{\kappa}$ and $\delta\tilde{\gamma}$ to the additional convergence and shear $\delta\kappa^{P,S}$ and $\delta\gamma^{P,S}$ coming from the lensing effect of the structure on a source S (S can be i, j or k):

$$\delta\kappa^{P,S} = \frac{D_{OL^P}}{D_{OL}}\frac{D_{L^PS}}{D_{0S}}\,\delta\tilde{\kappa} \tag{31}$$

$$\delta\gamma^{P,S} = \frac{D_{OL^P}}{D_{OL}}\frac{D_{L^PS}}{D_{OS}}\,\delta\tilde{\gamma}\,, \tag{32}$$

where the superscript ^{P} denotes the perturbative term. We assume that the convergence and the shear are constant all over the image. The shift produced by the linear lensing effect of the background structure (along the gradient of G), $\Delta^{LBS}_{\Omega,\lambda}$, on the cosmological parameters determination is then:

$$\Delta^{LBS}_{\Omega,\lambda} = \frac{\left\langle \begin{vmatrix} 1 & \omega_i & \frac{D_{L^Pj}}{D_{Lj}}\frac{D_{L^Pk}}{D_{Lk}} \\ 1 & \omega_j & \frac{D_{L^Pk}}{D_{Lk}}\frac{D_{L^Pi}}{D_{Li}} \\ 1 & \omega_k & \frac{D_{L^Pi}}{D_{Li}}\frac{D_{L^Pj}}{D_{Lj}} \end{vmatrix} \right\rangle \left(\frac{D_{OL^P}}{D_{OL}}\right)^2}{\left\| \nabla_{\Omega_0,\lambda_0} \left\langle \begin{vmatrix} 1 & \omega_i & \omega_i/\omega_i^o \\ 1 & \omega_j & \omega_j/\omega_j^o \\ 1 & \omega_k & \omega_k/\omega_k^o \end{vmatrix} \right\rangle \right\|} \left(\frac{\delta\tilde{\gamma}}{\gamma_\infty}\right)^2 . \tag{33}$$

For a condensation of mass located at redshift 1 and with the redshift distribution (39) this systematic is: $\Delta^{LBS}_{\Omega,\lambda} = 1.8\left(\frac{\delta\tilde{\gamma}}{\gamma_\infty}\right)^2$. To generalize this systematics to large scale structures, $\Delta^{LBS}_{\Omega,\lambda}$ has to be integrated along the line of sight. Here we do not perform exactly this calculation (which needs the introduction of cosmological scenario and the non linear evolution of perturbations) but only give an estimation of it using the already known results from the studies of lensing by large scale structures (see the review by Mellier 1998). Calculations from the non linear evolutions of the power spectrum on arc-minute scales predict a polarization of about 3%. From this value we can make a rough estimate of the shift on (Ω, λ) (using the same conditions as will be used in the simulations, Sect. 6): $\Delta^{LBS}_{\Omega,\lambda} \approx 0.03$. Better quantitative estimate of the amplitude of this systematics needs complete numerical simulations of the non-linear evolution of perturbations.

4.3.2. The multiplicative coupling term

The shift (along the gradient of G) due to the coupling effect of a background perturbing structure (with the main lens), $\Delta^{CBS}_{\Omega,\lambda}$, on the cosmological parameters determination is calculated as in 4.2.2. It is simpler since there is only one perturbating lens to which we associate an absolute convergence and shear (see Eq. (66)):

$$\Delta^{CBS}_{\Omega,\lambda} = \frac{\left\langle \begin{vmatrix} 1 & \omega_i & \frac{D_{L^Pi}}{D_{OL}}\left(\frac{D_{OL^P}}{D_{Oi}} - \frac{D_{LL^P}}{D_{Li}}\right) \\ 1 & \omega_j & \frac{D_{L^Pj}}{D_{OL}}\left(\frac{D_{OL^P}}{D_{Oj}} - \frac{D_{LL^P}}{D_{Lj}}\right) \\ 1 & \omega_k & \frac{D_{L^Pk}}{D_{OL}}\left(\frac{D_{OL^P}}{D_{Ok}} - \frac{D_{LL^P}}{D_{Lk}}\right) \end{vmatrix} \right\rangle}{\left\| \nabla_{\Omega_0,\lambda_0} \left\langle \begin{vmatrix} 1 & \omega_i & \omega_i/\omega_i^o \\ 1 & \omega_j & \omega_j/\omega_j^o \\ 1 & \omega_k & \omega_k/\omega_k^o \end{vmatrix} \right\rangle \right\|} \delta\tilde{\kappa}. \tag{34}$$

The same discussion as above applies. For a condensation of mass located at redshift 1 and with the redshift distribution (39) this systematic is: $\Delta^{CBS}_{\Omega,\lambda} = 16.7\delta\tilde{\kappa}$. To generalize this systematic to large scale structures, $\Delta^{CBS}_{\Omega,\lambda}$ has to be integrated along the line of sight. Instead, we use again a polarization of about 3% as in the previous section. However, contrary to the other two systematics, $\Delta^{GGL}_{\Omega,\lambda}$ and $\Delta^{LBS}_{\Omega,\lambda}$, $\Delta^{CBS}_{\Omega,\lambda}$ cannot be corrected because it behaves like a statistic noise, since $\delta\tilde{\kappa}$ can be either positive or negative. Its effect can only be minimized by adding a large number of clusters to the sample, so that we expect the averaged value of this systematic to behave roughly as the inverse of the square root of the number of considered clusters. As an example, for 100 clusters, we expect this systematic to be about $\Delta^{CBS}_{\Omega,\lambda} \approx 0.04$.

4.3.3. Effect of a background cluster

In the last two sections we discussed the non-linear evolution of background structures on scale of about one arcminute to estimate the resulting systematics on the triplet statistics. It may be also important to take in account (statistically) the effect of massive background clusters. In particular, the fortuitous presence of dense condensation of matter lying along the line of sight of the main lensing-cluster could be a serious artifact. Clusters of galaxies can be easily removed from the sample by using photometric redshift informations. However, if it happens that dark clusters exist then their presence could be more difficult to detect. Their impact on the statistics depend on their mass function which, in principle, can be obtained by using the aperture mass analysis proposed by Schneider (1996). This technique is able to detect a dark halo with velocity dispersion is larger than $600\,\mathrm{km\,s^{-1}}$ and has already proven that it is able to detect

blindly condensations of dark matter (see the recent detection of a dark cluster candidate by Erben et al. 1999).

Detailed quantitative estimates of the amplitude of the effect and the fraction of lensing clusters which is contaminated by another cluster along the line of sight require simulations as well as additional observations. This study is beyond the scope of this paper, but should be addressed in a forthcoming paper. It is also worth noting again that, if this fraction is small, then it is certainly better to remove from the sample all the targets which seem to be contaminated.

4.4. Outcome

Estimations of the various systematic biases are given in the following table, for a principal lens at redshift 0.4, and a redshift distribution similar to (38):

Next section will give qualitative solutions to deal with part of these systematics and to increase the signal to noise ratio of the method.

5. Optimization of the triplet statistics

So far, the method has been presented in a general way, with no particular choice for the geometry of clusters, neither for the redshifts nor for the distances between galaxies inside triplets. This section discusses qualitatively these degrees of freedom in order to increase the signal and decrease the bias $\Delta^{LBS}_{\Omega,\lambda}$.

5.1. Choosing clusters with symmetrical geometry

The triplet statistics as explained so far can be applied to any clusters regardless their geometry. However, it can be optimized by selecting those having interesting properties, like clusters having mass density contours with symmetrical geometry. Simple geometry permits to define narrow strips around clusters which follow the mass density and where each galaxy experiences the same gravitational potential. Therefore, galaxies inside a strip can be associated with more pairs of galaxies of the strip in order to define triplets. For clusters with elliptical shape, galaxies located at symmetric positions with respect to the cluster center can be used jointly. An extreme case is the circular cluster where any triplet formed with galaxies located inside the strip can be used. These lensing configurations can significantly increase the number of triplets and permit to use those with large angular separation, which suppresses some systematics discussed in the previous sections.

In particular, the systematic bias produced by the linear perturbation effect of background structures (see Sect. 4.3.1) can be significantly reduced. This bias is due to scalar products as $\boldsymbol{g}^{P,i}\boldsymbol{g}^{P,j*}$ appearing from the construction of G_{ijk} in the determinant:

$$\begin{vmatrix} 1 & \omega_i^o & \omega_i^o \boldsymbol{g}^{P,j}\boldsymbol{g}^{P,k*} \\ 1 & \omega_j^o & \omega_j^o \boldsymbol{g}^{P,k}\boldsymbol{g}^{P,i*} \\ 1 & \omega_k^o & \omega_k^o \boldsymbol{g}^{P,i}\boldsymbol{g}^{P,j*} \end{vmatrix}. \tag{35}$$

Assume that we apply the triplet statistics to a circular cluster. We can construct a sub-sample of triplets of galaxies inside a ring centered on the cluster center. Each galaxy (i, j or k) of the triplet is associated with an angle, $\alpha_i, \alpha_j, \alpha_k$. Hence, we can replace each measured ellipticity ($\boldsymbol{\epsilon}_i, \boldsymbol{\epsilon}_j$ and $\boldsymbol{\epsilon}_k$) by the tangential ellipticities ($\boldsymbol{\epsilon}_i e^{2i\alpha_i}$, $\boldsymbol{\epsilon}_j e^{2i\alpha_j}$ and $\boldsymbol{\epsilon}_k e^{2i\alpha_k}$), so that the writes:

$$\begin{vmatrix} 1 & \omega_i^o & \omega_i^o \boldsymbol{g}^{P,j}\boldsymbol{g}^{P,k*} e^{2i(\alpha_j-\alpha_k)} \\ 1 & \omega_j^o & \omega_j^o \boldsymbol{g}^{P,k}\boldsymbol{g}^{P,i*} e^{2i(\alpha_k-\alpha_i)} \\ 1 & \omega_k^o & \omega_k^o \boldsymbol{g}^{P,i}\boldsymbol{g}^{P,j*} e^{2i(\alpha_i-\alpha_j)} \end{vmatrix}. \tag{36}$$

We can see that the arguments of the elements of the third column are randomly distributed. Therefore the systematic bias $\Delta^{LBS}_{\Omega,\lambda}$ vanishes as the inverse of the square root of the number of triplets whereas the main term is not modified.

The signal to noise ratio of the method (as defined in (25)) can also be increased because the number of triplets becomes large enough to enable a stringent selection taking into account the environment of the three sources (see 5.2), or their redshift (see 5.3.1).

The optimization of the selection of clusters is difficult today because the number of lensing clusters with good geometrical properties is a tiny fraction of the samples. However in the near future we expect many new cluster samples coming out from dedicated surveys. For example, the new sample obtained by the X-ray satellite XMM, will be useful to select many clusters having the most regular and symmetrical shape, like cD-clusters of galaxies.

5.2. Choosing the triplets of galaxies

It is also possible to reject from the sample the sources for which another galaxy may play the role of a galaxy lens. The angular radius of the circle in which we can consider that a galaxy is isolated without important local perturbation of another galaxy depends on the real mass distribution of galaxy halos. Therefore it is somewhat difficult to provide accurate estimate of this circle with our present-day knowledge of the distant galaxy halos. As a rough simplification we can consider each galaxy as an isothermal sphere and then choose the angular radius such that the induced shear (and convergence) is lower than 5%. This conservative approximation applies not only in the Sect. 4.2.1, but also in 4.2.2, where $\tilde{\kappa}^{gal}$ can thus be chosen small ($\approx 2\%$) in order to decrease the systematic bias $\Delta^{GGL}_{\Omega,\lambda}$.

Of equal importance is the question of the maximum distance Δr tolerable between each component of the triplet. Or, in the case of a circular cluster analysis, what is the acceptable thickness of the rings? To answer we need to balance two opposite effects: first, while Δr increases, $\langle\gamma_\infty\rangle$ decreases proportionally to about $1-\Delta r/r$ (if the shear of the cluster is a law in $1/r$, as for an isothermal sphere), so the signal to noise ratio decreases; second, in the same time the number of triplets increases making possible a judicious selection of the redshifts in the triplets (see Sect. 5.3.1). After realistic simulations (using a number density of galaxies equal to 50 galaxies arcmin^{-2}), the optimized value that has been selected for the first presentation of the method is 20 arcseconds separation. In practice, this can be optimized accordingly to the shear map of the cluster.

5.3. Redshift optimization

In this section we suppose that the redshift distribution $n(z)$ and the variance of the redshift error $\sigma_{\Delta z}(z)$ are known. We then investigate if the signal to noise ratio of the method can be improved thanks to either a choice in the redshifts of the triplets or a selection in redshift of the clusters. In all the oncoming considerations the number density of background galaxies has been taken equal to 50 galaxies arcmin^{-2}).

5.3.1. Redshifts in triplets

From the matrix form (15), it appears obvious that if two of the three redshifts of a triplet are very close together then the resulting value of G_{ijk}^{main} is nearly zero and thus does not provide any cosmological information to G. In reality, such degenerated triplets decrease the cosmological signal (G^{main}) -they introduce G_{ijk}^{main} terms equal to zero in the average of G- but do not change the nature of the noise: even if a triplet is degenerated in redshift, the associated N_{ijk} term always have a random signature.

This effect is particularly critical in the areas where a large clustering of galaxies is detected. Therefore it is necessary to set two minimum redshift differences $\Delta_{ij} = z_j - z_i$ and $\Delta_{jk} = z_k - z_j$ below which the triplets will not be rejected. On the other hand, if these minima are too high then too many triplets will be rejected, increasing the terms $1/\sqrt{N}$ and σ_{GN}. The right balance is obtained for Δ_{ij} and Δ_{jk} greater than about 0.05.

This small value has been obtained from simulations. It proves that in the balance, the second effect is stronger. It means that with this density of galaxies, any stringent selection makes σ_{GN} rapidly decreasing. This will not be true anymore if we can select triplets within rings, for a nearly circular cluster, or if we use observations with NGST (which will increase significantly the number density of galaxies). In these two cases, the balance becomes favorable to selections and so to an increase of the signal to noise ratio of the estimator.

The second concern about the redshift selection is the difference between z_i and the redshift of the lens, Δ_{li}. Once again, the optimization arises with the balance of two competing effects: if z_i is too close to z_l then the noise is increased by a nearly infinite value of $\Delta\omega_i$; however, in the same time the gradient of G_{ijk}^{main} is greater. Our simulations show that the right balance is obtained for Δ_{li} greater than about 0.05, and the same discussion as above applies.

5.3.2. Redshifts of clusters

We can also find the best balance between the last two effects when the redshift of the cluster changes. The most favorable cluster redshifts are strongly dependent on the shape of $\sigma_{\Delta z}(z)$: the redshift of the cluster must be in the area where the errors on the redshifts are as small as possible for $\Delta\omega_i$ to be non dominant in the signal to noise ratio.

Besides, if the redshift of the cluster is too low then $\omega_i \approx \omega_j \approx \omega_k$ whatever the triplet is, the S/N decreases.

With $\sigma_{\Delta z}(z)$ approximately equal to 0.03 for redshift inferior to 0.8 and equal to 0.1 for other redshifts, simulations show that clusters at redshift between 0.3 and 0.5 are the most favorable to the method.

6. Simulations and results

In the simulations, we assumed that the redshift of each galaxy was known and we took a redshift distribution $n(z)$ which represents both the usual peak of galaxies near $z = 1$ (described by the redshift distribution $p(z)$ from Brainerd et al. 1996) as well as a more distant population of faint blue galaxies suggested by deep multicolor observations (see Fort et al. 1996, Broadhurst 1998):

$$n(z) = \alpha_1 p(z) + \alpha_2 p(z-2) \text{ with} \tag{37}$$

$$p(z) = \frac{\beta z^2}{\Gamma\left(\frac{3}{\beta}\right) z_0^3} \exp\left[-\left(\frac{z}{z_0}\right)^{\beta}\right] , \tag{38}$$

with $z_0 = 1/3$ and $\beta = 1$, the $p(z)$ and $p(z-2)$ distributions give respectively an average redshift equal to 1 and 3. With $\alpha_1 = 0.7$ and $\alpha_2 = 0.3$, the fraction of high and low redshift galaxies found by Fort et al. in the field of the lensing-cluster Cl0024+1654 is reproduced. Although Broadhurst seems to have confirmed the result of this observation with the Keck telescope (T. Broadhurst, private communication), the redshift distribution may not be exactly representative of the general redshift distribution of the faint galaxy population for which we can determine good color redshift. However, it is important to remember that the triplet statistics actually test the convexity of the lensing factor curve $\omega(z)$ (see Fig. 1). Therefore, its accuracy mostly depends on the total number of galaxies above $z = 1$ that we can detect and for which we can determine an accurate color redshift (high signal to noise for B photometry is essential). If a deep multicolor photometry from U to K gives a broader redshift distribution with more galaxies at intermediate redshift ($z = 1.5$–2) the result of the triplet statistics will be better since the new distribution will increase the number of possible triplets with significant information on the cosmology.

In the redshift simulations the clustering effects were not taken in account (each redshift was chosen separately). This simplification was discussed in Sect. 5.3.1. A further paper will account for the clustering effects in order to evaluate the effect of this simplification on the signal to noise ratio of the method and to estimate the systematics due to the background structures (multi-lensing effects. see 4.2) created from the clustering of galaxies.

We have also put realistic uncertainties in the photometric redshift of galaxies. We assume it is a Gaussian distribution with a redshift dispersion equal to 0.03 for redshifts lower than 0.8 and as large as 0.1 for redshifts greater than 0.8 (see Brunner et al. 1997 and Hogg et al. 1998).

The intrinsic ellipticity distribution is chosen as follows:

$$p_{\boldsymbol{\epsilon}_S}(\boldsymbol{\epsilon}_S) = \frac{1}{\pi\sigma_{\epsilon_S}^2\left(1 - e^{-1/\sigma_{\epsilon_S}^2}\right)} \exp\left[-\left(\frac{\epsilon_S}{\sigma_{\epsilon_S}}\right)^2\right] \tag{39}$$

with the intrinsic ellipticity dispersion $\sigma_{\epsilon_S} = 0.15$ (from Seitz & Schneider 1997).

For errors on the measured ellipticities, we chose the same distribution, with a dispersion equal to 0.02.

For the clusters, the redshift have been taken equal to 0.4, and their projected mass density has the following analytical shape:

$$\kappa(r, \theta) = \frac{\kappa_o}{r\sqrt{1 + e\cos 2\theta}}. \quad (40)$$

The cluster ellipticities were chosen randomly between 0 and 0.5. It is unimportant to include a core radius since its influence in the weak lensing area is negligible (in principle, the triplet statistics cancels any dependency on the mass map of the cluster). κ_o is taken to correspond to a sample of high velocity dispersion ($1000\,\mathrm{km\,s^{-1}}$).

The size of the observation window has been taken similar to what will give the VLT instrument FORS: $6' \times 6'$. Within this window, a circle of $90''$ radius representing the arclets and strong lensing regimes was not considered.

So, with an average of about 50 galaxies arcmin^{-2}, each VLT observation of a cluster contains about 1000 background galaxies.

Now, the question we address with the simulations is: what is the accuracy we can reach on the cosmological parameters for a given number of observed clusters?

Fig. 4 gives the contours $p_{\Omega,\lambda}(\Omega, \lambda)$ for simulations concerning 1000 clusters in three cases: first case, $\Omega_o = 0.3$ and $\lambda_o = 0.7$; second case, $\Omega_o = 0.3$ and $\lambda_o = 0$; third case, $\Omega_o = 1$ and $\lambda_o = 0$. Fig. 5 gives the same for 100 clusters.

The results of these simulations are promising. They prove that with only 100 clusters $\lambda^{+0.3}_{-0.2}$ (in the case $\Omega + \lambda = 1$) and $\Omega^{+0.30}_{-0.25}$ (in the case $\lambda = 0$) can be reached (with a 70% confidence level). This number corresponds to about 20 nights of VLT observation. $\Omega = 0.3$ and $\Omega = 1$ universes can also be separated at a $2\sigma = 95\%$ confidence level with the same time of observation: about 20 VLT nights. Therefore, even a modest observing campaign on a VLT could provide interesting constraints on λ.

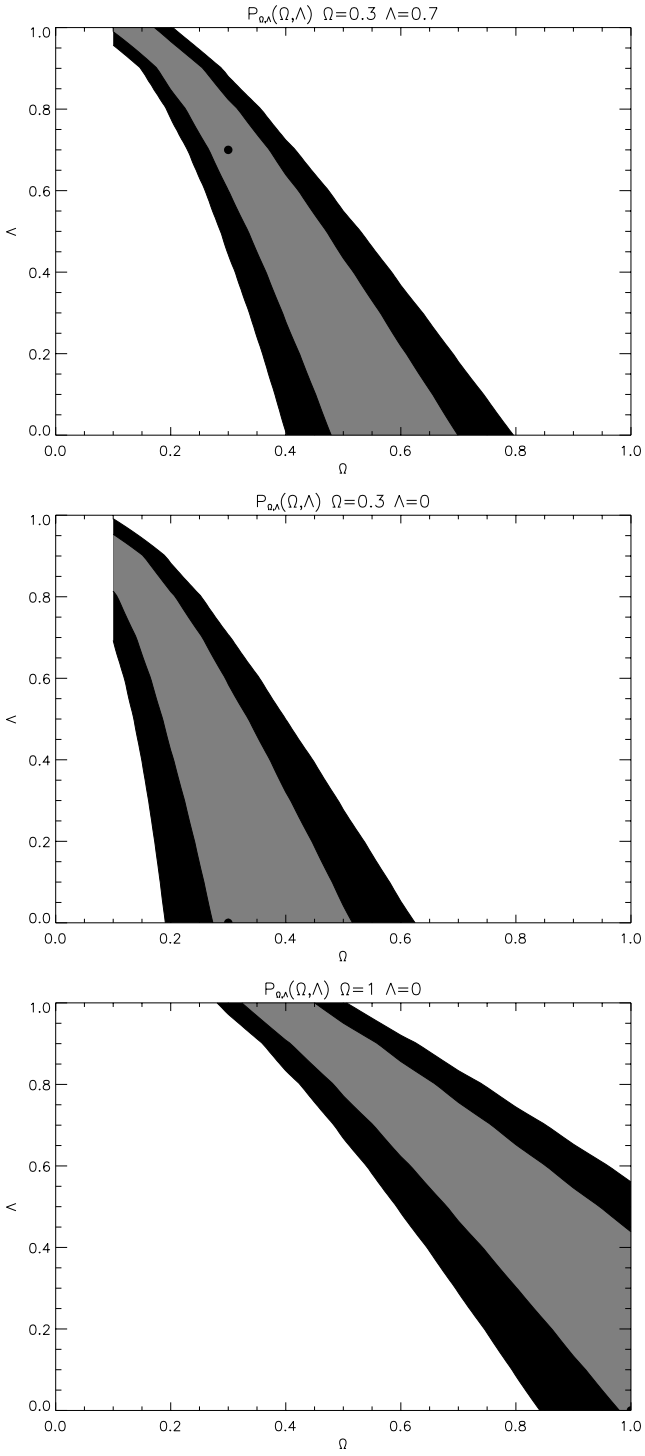

Fig. 4. Contours of the (Ω, λ) probability distribution obtained from a simulation on 1000 clusters in the cases $(\Omega, \lambda) = (0.3, 0.7)$ (top panel), $(\Omega, \lambda) = (0.3, 0)$ (middle panel) and $(1, 0)$ (bottom panel). We give the $1\sigma = 68\%$ (grey) and $2\sigma = 95\%$ (dark) confidence levels.

7. Conclusion

We have presented a new test to constrain the cosmological parameters (Ω, λ), the triplet statistics. It is based on the comparison of the gravitational distortion produced by a cluster of galaxies on triplets of neighboring galaxies having different (photometric) redshift but which experience the gravitational potential at the same position. This purely geometrical test is therefore insensitive to the lens modeling and can be directly applied to real data using the ellipticities of galaxies as observed from optical images. We have shown that the statistical noise of the triplet statistics is dominated by the intrinsic source ellipticity.

The main result is that with a short program of observations (about 20 VLT nights) a constraint on the value of the cosmological constant could be obtained. Using the observation of 100 clusters, we can reach $\lambda^{+0.3}_{-0.2}$ in the case $\Omega + \lambda = 1$ or $\Omega^{+0.3}_{-0.25}$ in the case $\lambda = 0$ (at a 1σ level). These results could be even refined down to 10% accuracy on (Ω, λ) with the use of NGST. Indeed, this telescope looks perfectly suited for this

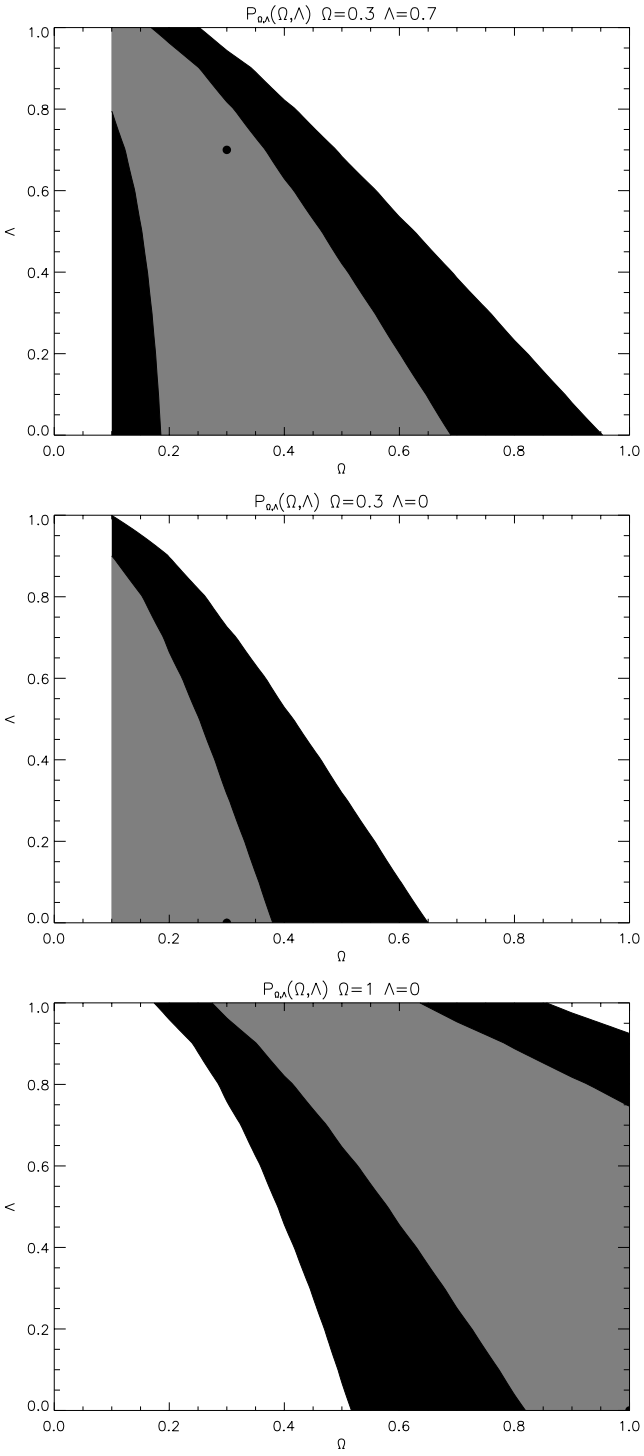

Fig. 5. Contours of the (Ω, λ) probability distribution obtained from a simulation on 100 clusters in the cases $(\Omega, \lambda) = (0.3, 0.7)$ (top panel), $(\Omega, \lambda) = (0.3, 0)$ (middle panel) and $(1, 0)$ (bottom panel). We give the $1\sigma = 68\%$ (grey) and $2\sigma = 95\%$ (dark) confidence levels.

method since it considerably increases the number density of observed background galaxies.

Though the paper is devoted to the description of the principle of the method, we discussed the main systematic biases. We have estimated the amplitude of the systematics due to the presence of background structures with a multi-lensing model. It turns out that the shifts on the (Ω, λ) determination are about 0.05. Some of the systematics can be directly corrected: the perturbative effect due to galaxy-galaxy lensing and the effect of background structures integrated along the line of sight. A detailed estimation of the correction requires calculations that take in account the non linear evolution of large scale structures. Numerical simulations including cosmological scenario of structure formation with introduction of large scale structures, and in particular the introduction of clustering effects, are therefore necessary to validate the method.

In conclusion, we have shown that the systematic effects could be well controlled by a judicious selection criteria of the clusters and the lensed galaxies of each triplet.

The (Ω, λ) degeneracy of the triplet statistics is orthogonal to the one of the classical (m, z) of supernovae searches. In this regards, when combined to the supernovae approach, the triplet statistics using VLT or NGST data could be extremely efficient.

More generally, it is important to investigate thoroughly the possibility to use cluster lenses as observational tests to constrain the curvature of the Universe. Clusters produce strong effects as compare to galaxy lenses (large angular scale effects, strong magnification). They distort a large population of distant background sources whose redshift distribution can be well known from (future) spectroscopic surveys and photometric redshift techniques. Big telescopes with high image quality, like the VLT and latter the NGST, are the best suited instruments for these programs.

Acknowledgements. We thank F. Bernardeau and L. van Waerbeke for fruitful discussions and their useful comments. This work was supported by the Programme National de Cosmologie.

Appendix A: the observed ellipticity of a background source

We remind the practical way to calculate the image ellipticity $\boldsymbol{\epsilon}_I = \epsilon_I e^{2i\theta_I}$ of a source from the image of a galaxy as a function of $\boldsymbol{g} = \frac{\boldsymbol{\gamma}}{1-\kappa}$).

In the following, the local convergence is κ, the complex shear is $\boldsymbol{\gamma} = \gamma e^{2i\theta_L}$ and the intrinsic source ellipticity $\boldsymbol{\epsilon}_S = \epsilon_S e^{2i\theta_S}$.

For each background galaxy we can calculate a second moment matrix M^I. Then the complex image ellipticity is derived from the second moments (see Seitz & Schneider 1997):

$$\boldsymbol{\epsilon}_I = \frac{M^I_{11} - M^I_{22} + 2iM^I_{12}}{M^I_{11} + M^I_{22} + 2\sqrt{det(M^I)}}. \quad \text{(A.1)}$$

This definition is consistent with Eq. (5). We also use a second order momentum matrix M^S for the source as it would be seen with no lens.

The effect of the lens on the ellipticity of the background galaxy can then be summarized in the matrix Eq. (see Bonnet 1995):

$$M^I = \frac{AM^S{}^t A}{|A|^2} \text{ with} \quad \text{(A.2)}$$

$$A = \frac{(1-\kappa)I^0 + \gamma J^{2\theta}}{(1-\kappa)^2 - \gamma^2}. \quad \text{(A.3)}$$

In what follows and above, we use the notations

$$I^{2\theta} = \begin{pmatrix} \cos(2\theta) & -\sin(2\theta) \\ \sin(2\theta) & \cos(2\theta) \end{pmatrix}, \quad \text{(A.4)}$$

$$J^{2\theta} = \begin{pmatrix} \cos(2\theta) & \sin(2\theta) \\ \sin(2\theta) & -\cos(2\theta) \end{pmatrix}. \quad \text{(A.5)}$$

Eq. (A2) leads to

$$M^I = \frac{(I^0 + gJ^{2\theta})I^\theta \begin{pmatrix} \frac{1+\epsilon}{1-\epsilon} & 0 \\ 0 & \frac{1-\epsilon}{1+\epsilon} \end{pmatrix} I^{-\theta}(I^0 + gJ^{2\theta})}{|1-g^2|}. \quad \text{(A.6)}$$

Using the following properties:

$$J^\alpha J^\beta = I^{\alpha-\beta},\ J^\alpha I^\beta = J^{\alpha-\beta},\ I^\alpha J^\beta = J^{\alpha+\beta}, \quad \text{(A.7)}$$

Eq. (A7) gives:

$$\begin{aligned} |1-g^2|(1-\epsilon_S^2)\ M^I = \ & (1+\epsilon_S^2)(1+g^2) \\ & +4g\epsilon_S \cos(2(\theta_S - \theta_L))]I^0 \\ & +2\epsilon_S J^{2\theta_S} + 2g(1+\epsilon_S^2)J^{2\theta_L} \\ & +2g^2\epsilon_S J^{4\theta_L - 2\theta_S}. \end{aligned} \quad \text{(A.8)}$$

Finally, whatever the value of g is (meaningly either in the weak or strong lensing regime) the measured image ellipticity writes:

$$\boldsymbol{\epsilon}_I = \frac{\boldsymbol{\epsilon}_S + (1+\epsilon_S^2)\boldsymbol{g} + \boldsymbol{\epsilon}_S^* \boldsymbol{g}^2}{max(1, g^2) + \epsilon_S^2 min(1, g^2) + \boldsymbol{\epsilon}_S^* \boldsymbol{g} + \boldsymbol{\epsilon}_S \boldsymbol{g}^*}, \quad \text{(A.9)}$$

which, in the weak lensing and arclet regimes ($g < 1$) simplifies into (to the third order in ϵ_S and g):

$$\boldsymbol{\epsilon}_I = (1-g^2)\boldsymbol{\epsilon}_S + \boldsymbol{g} - \boldsymbol{g}^* \boldsymbol{\epsilon}_S^2, \quad \text{(A.10)}$$

where the term $\boldsymbol{g}^* \boldsymbol{\epsilon}_S^2$ is negligible regarding to the term $\boldsymbol{\epsilon}_S$ and vanishes in $1/\sqrt{N}$ (because the argument of this term behaves randomly) in the operator G as the different noises described in Sect. 3.4. Therefore the final equation for the image ellipticity writes:

$$\boldsymbol{\epsilon}_I = (1-g^2)\boldsymbol{\epsilon}_S + \boldsymbol{g}. \quad \text{(A.11)}$$

It is worth noticing that the term $(1-g^2)$ supports favourably the test developed in this paper. With the conditions used in the simulations (Sect. 6), the mean value of this term is about 0.85. It means that the noise coming from the intrinsic source ellipticity is lowered by 15% or, for a given signal to noise ratio, the number of required clusters is lowered by 28%.

Appendix B: the case of a perturbing lens

In this appendix, we estimate the influence of a perturbative lens (galaxy, cluster or higher scale structure) located behind the principal lensing cluster on the measured ellipticity of a background source.

The calculation of the total amplification matrix in the case of two (or more) consecutive lenses has already been done (see for example Kovner 1997). The result can be simply noticed as follows:

$$A^{-1} = I^0 - L - L^P + cL^P L \text{ with} \quad \text{(B.1)}$$

$$L = \kappa I^O + \gamma J^{2\theta_L} \text{ and} \quad \text{(B.2)}$$

$$L^P = \kappa^P I^O + \gamma^P J^{2\theta_P}. \quad \text{(B.3)}$$

The ^{P} upper index refers to the perturbative lens. The c coupling factor is $c = \frac{D_{LL^P} D_{OS}}{D_{OL^P} D_{LS}}$.

Eq. (B2) rewrites:

$$\begin{aligned} A^{-1} = \ & (1-\kappa-\kappa^P + c\kappa\kappa^P)I^0 - \gamma(1-c\kappa^P)J^{2\theta_L} \\ & -\gamma^P(1-c\kappa)J^{2\theta_P} + c\gamma\gamma^P I^{2(\theta_P - \theta_L)}, \end{aligned} \quad \text{(B.4)}$$

which can be inverted into

$$\begin{aligned} A = \ & \frac{1}{|A^{-1}|}[(1-\kappa-\kappa^P + c\kappa\kappa^P)I^0 + \gamma(1-c\kappa^P)J^{2\theta_L} \\ & +\gamma^P(1-c\kappa)J^{2\theta_P} + c\gamma\gamma^P I^{2(\theta_L - \theta_P)}]. \end{aligned} \quad \text{(B.5)}$$

Unlike a single lens, the amplification matrix has an anti-symmetric term (the last one of Eq. (B6)). However, the amplification matrix still transforms an ellipse of the source plane into another ellipse in the image plane. We thus can search for the image ellipticity of a source distorted by both lenses, as a function of the source ellipticity and the potential of the principal and perturbative lenses. We proceed the same way as in annex A.

In the following, we only keep second order terms in $\kappa, \kappa^P, \gamma, \gamma^P$ and ϵ_S. So we can use the definitions:

$$\tilde{\boldsymbol{g}} = (1-\kappa-(1-c)\kappa^P)^{-1}\boldsymbol{\gamma} \quad \text{(B.6)}$$

$$\tilde{\boldsymbol{g}}^P = (1-(1-c)\kappa-\kappa^P)^{-1}\boldsymbol{\gamma}^P\ , \quad \text{(B.7)}$$

and rewrite the amplification matrix:

$$A = \frac{I^0 + \tilde{g}J^{2\theta_L} + \tilde{g}^P J^{2\theta_P} + c\tilde{g}\tilde{g}^P I^{2(\theta_L - \theta_P)}}{1-\tilde{g}^2 - \tilde{g}^{P2} - 2(1-c)Re(\tilde{g}\tilde{g}^{P*})}. \quad \text{(B.8)}$$

Finally, with a calculation similar to the one done in annex A, we obtain for the image ellipticity:

$$\begin{aligned} \boldsymbol{\epsilon}_I = \ & (1-|\tilde{\boldsymbol{g}} + \tilde{\boldsymbol{g}}^P|^2)\boldsymbol{\epsilon}_S + \tilde{\boldsymbol{g}} + \tilde{\boldsymbol{g}}^P - 4cRe\left[(\tilde{\boldsymbol{g}}\tilde{\boldsymbol{g}}^{P*}(\tilde{\boldsymbol{g}} + \tilde{\boldsymbol{g}}^P)\right. \\ & \left. -2c\tilde{\boldsymbol{g}}^*\tilde{\boldsymbol{g}}^P\boldsymbol{\epsilon}_S - \epsilon_S^2(\tilde{\boldsymbol{g}}^* + \tilde{\boldsymbol{g}}^{P*})\right] \end{aligned} \quad \text{(B.9)}$$

which we simplify into

$$\boldsymbol{\epsilon}_I = \left(1-|\tilde{\boldsymbol{g}} + \tilde{\boldsymbol{g}}^P|^2\right)\boldsymbol{\epsilon}_S + \tilde{\boldsymbol{g}} + \tilde{\boldsymbol{g}}^P\ , \quad \text{(B.10)}$$

where we have cancelled all the terms higher to the second order and oriented randomly (we consider that the source ellipticity, the principal and perturbative shears are independent. Terms higher to the second order with a random orientation give a negligible noise -regarding to the noise coming from the intrinsic source ellipticity- in the calculation of G).

Comparing Eqs. (A11) and (B10) we can see the effect of the perturbative lens on the measured ellipticity:

1. a complex additive correction $\tilde{\boldsymbol{g}}^P$ which orientation is non correlated to the one of the cosmological term,

2. a scalar correction $(1-c)\kappa^P$ on the cosmological term $\boldsymbol{g}$, due to coupling between the main and the perturbative lenses.

The simple form of Eq. (B10) can be easily generalized to the case of a succession of many lenses noticed L^0 (instead of the principal lens), L^1 (instead of the perturbative lens), L^2,..., L^n between the observer and the source noticed S. If the coupling factor between the lenses i and j (with $z_i < z^j$) is noticed $c^S_{i,j} = \frac{D_{OS}D_{L^iL^j}}{D_{OL_j}D_{L_iS}}$, then Eq. (A11) giving the amplification matrix can be generalized into:

$$A^{-1} = \bigotimes_{i=n}^{i=0}(I^0 - L^i) = (I^0 - L^n) \otimes ... \otimes (I^0 - L^0), \quad \text{(B.11)}$$

where the $\otimes$ symbol defines a particular matrix product with the following properties: $I^0 \otimes L^i = L^i \otimes I^0 = L^i$, $L^j \otimes L^i = c^S_{i,j}L^jL^i$, $L^k \otimes L^j \otimes L^i = c^S_{i,j}c^S_{j,k}L^kL^jL^i$ etc...

We can remark that in the case of two very close lenses, their associated coupling factor c is zero. With the same calculations and approximations as above we obtain:

$$\boldsymbol{\epsilon}_I = \left(1 - |\sum_{i=0}^{i=n}\tilde{\boldsymbol{g}}^i|^2\right)\boldsymbol{\epsilon}_S + \sum_{i=0}^{i=n}\tilde{\boldsymbol{g}}^i \text{ with} \quad \text{(B.12)}$$

$$\tilde{\boldsymbol{g}}^i = \left(1 - \kappa^i - \sum_{j\neq i}(1 - c^S_{i,j})\kappa^j\right)^{-1}\gamma^i. \quad \text{(B.13)}$$

Appendix C: the noise and the main terms in the construction of G

This appendix explains the form of the G_{ijk} term and prove Eq. (12). The noise terms N_{ijk} and GN are then derived from a budget error analysis which takes into account the uncertainties of the measurements (including redshifts and ellipticities of the background galaxies). We finally prove that, for a large number of triplets, the terms N_{ijk} are randomly distributed and therefore the average term GN is indeed a noise that converges to zero.

Let us first consider a triplet of close background sources. It is composed of two set of observable quantities which also form triplets: $(\boldsymbol{\epsilon}_i, \boldsymbol{\epsilon}_j, \boldsymbol{\epsilon}_k)$, for the associated measured ellipticities, and (z_i, z_j, z_k), for the associated redshifts (that we assume they are obtained from photometric redshifts). For convenience, instead of the redshifts we will use the associated lens factors $(\omega_i, \omega_j, \omega_k)$ (see Eq. (9) for their definition). Because of measurement errors, each of these observable quantities may differ from the actual ellipticities and redshifts. We introduce these errors as $\Delta\boldsymbol{\epsilon}$ and Δz (associated to $\Delta\omega$), that we will also index by i, j or k. Besides, because the light of the three neighboring galaxies does not exactly cross the lens plane at the same position, the quantities derived from the lens potential, κ_∞ and $\boldsymbol{\gamma}_\infty$, are not exactly the same for all the three galaxies. We will then also index these quantities by i, j or k and will notice κ_∞ and $\boldsymbol{\gamma}_\infty$ their averaged values. The shift between $\kappa_{\infty,s}$ and κ_∞ will be noticed $\Delta\kappa_{\infty,s}$ ($s = i, j$ or k). Similar definition and notations apply for $\Delta\boldsymbol{\gamma}_{\infty,s}$ ($s = i, j$ or k).

We can now rewrite exactly the Eq. (10) (in the following we use the lower index i, but the calculation is valid to the indexes j or k):

$$\boldsymbol{\epsilon}_i = \bar{\boldsymbol{\epsilon}}_{S,i} + \Delta\boldsymbol{\epsilon}_{S,i} + \tilde{\boldsymbol{g}_i^o} \text{ with} \quad \text{(C.1)}$$

$$\tilde{\boldsymbol{g}_i^o} = \frac{\omega_i^o(\boldsymbol{\gamma}_\infty + \Delta\boldsymbol{\gamma}_{\infty,i})}{1 - \omega_i^o(\kappa_\infty + \Delta\kappa_{\infty,i})}. \quad \text{(C.2)}$$

The term $\tilde{\boldsymbol{g}_i^o}$ slightly differs from the main cosmological term $\boldsymbol{g}_i^o$ which is given in Eq. (11). The noise N_{ijk} is the difference between those two terms. To first order in $\Delta\boldsymbol{\gamma}_{\infty,i}$ and $\Delta\kappa_{\infty,i}$ it writes:

$$\boldsymbol{\epsilon}_i = \boldsymbol{g}_i^o + \bar{\boldsymbol{\epsilon}}_{S,i} + \Delta\boldsymbol{\epsilon}_{S,i} + \omega_i^o\Delta\boldsymbol{\gamma}_{\infty,i} \quad \text{(C.3)}$$

that we identify term to term to

$$\boldsymbol{\epsilon}_i = \tilde{\boldsymbol{g}_i^o} + \boldsymbol{p}_i^1 + \boldsymbol{p}_i^2 + \boldsymbol{p}_i^3 \quad \text{(C.4)}$$

where the $\boldsymbol{p}$ terms are the perturbative noises. The upper index refers to the different types of noises (see their description in Sect. 3.4). The lower index can be i, j or k depending on the galaxy of the triplet. They are all randomly distributed around zero when considering different triplets.

Similarly, since the measured redshifts are not the actual ones (in particular when they are obtained from photometric redshift techniques), the exact form of the measured G_{ijk} operator is

$$G_{ijk}(\Omega, \lambda) = \begin{vmatrix} 1 & \omega_i + \Delta\omega_i & (\omega_i + \Delta\omega_i)\boldsymbol{\epsilon}_j\boldsymbol{\epsilon}_k^* \\ 1 & \omega_j + \Delta\omega_j & (\omega_j + \Delta\omega_j)\boldsymbol{\epsilon}_k\boldsymbol{\epsilon}_i^* \\ 1 & \omega_k + \Delta\omega_k & (\omega_k + \Delta\omega_k)\boldsymbol{\epsilon}_i\boldsymbol{\epsilon}_j^* \end{vmatrix}, \quad \text{(C.5)}$$

which can be also written as

$$G_{ijk}(\Omega, \lambda) = T^0_{ijk} + T^1_{ijk} + T^2_{ijk} + T^3_{ijk} \quad \text{(C.6)}$$

where we noticed

$$T^0_{ijk} = \begin{vmatrix} 1 & \omega_i & \omega_i\boldsymbol{\epsilon}_j\boldsymbol{\epsilon}_k^* \\ 1 & \omega_j & \omega_j\boldsymbol{\epsilon}_k\boldsymbol{\epsilon}_i^* \\ 1 & \omega_k & \omega_k\boldsymbol{\epsilon}_i\boldsymbol{\epsilon}_j^* \end{vmatrix} \quad \text{(C.7)}$$

$$T^1_{ijk} = \begin{vmatrix} 1 & \omega_i & \Delta\omega_i\boldsymbol{\epsilon}_j\boldsymbol{\epsilon}_k^* \\ 1 & \omega_j & \Delta\omega_j\boldsymbol{\epsilon}_k\boldsymbol{\epsilon}_i^* \\ 1 & \omega_k & \Delta\omega_k\boldsymbol{\epsilon}_i\boldsymbol{\epsilon}_j^* \end{vmatrix} \quad \text{(C.8)}$$

$$T^2_{ijk} = \begin{vmatrix} 1 & \Delta\omega_i & \omega_i\boldsymbol{\epsilon}_j\boldsymbol{\epsilon}_k^* \\ 1 & \Delta\omega_j & \omega_j\boldsymbol{\epsilon}_k\boldsymbol{\epsilon}_i^* \\ 1 & \Delta\omega_k & \omega_k\boldsymbol{\epsilon}_i\boldsymbol{\epsilon}_j^* \end{vmatrix} \quad \text{(C.9)}$$

$$T^3_{ijk} = \begin{vmatrix} 1 & \Delta\omega_i & \Delta\omega_i\boldsymbol{\epsilon}_j\boldsymbol{\epsilon}_k^* \\ 1 & \Delta\omega_j & \Delta\omega_j\boldsymbol{\epsilon}_k\boldsymbol{\epsilon}_i^* \\ 1 & \Delta\omega_k & \Delta\omega_k\boldsymbol{\epsilon}_i\boldsymbol{\epsilon}_j^* \end{vmatrix}. \quad \text{(C.10)}$$

To express the noise term N_{ijk}, we first need to calculate all the quantities like

$$\boldsymbol{\epsilon}_j\boldsymbol{\epsilon}_k^* = g_j^o g_k^o + \sum_{n=1}^{3}(g_k^{o*}\boldsymbol{p}_j^n + g_k^o\boldsymbol{p}_j^{n*}) + \sum_{m,n=1}^{3}\boldsymbol{p}_j^n\boldsymbol{p}_k^{m*} \quad \text{(C.11)}$$

that we rewrite

$$\boldsymbol{\epsilon}_j \boldsymbol{\epsilon}_k^* = g_j^o g_k^o + n_{jk} \tag{C.12}$$

Using jointly Eqs. (C8) and (C12), we can now express G_{ijk} as function of the main and the noise terms (G_{ijk}^{main} and N_{ijk}):

$$G_{ijk} = G_{ijk}^{main} + N_{ijk} \tag{C.13}$$

$$G_{ijk}^{main} = \begin{vmatrix} 1 & \omega_i & \omega_i g_j^o g_k^o \\ 1 & \omega_j & \omega_j g_k^o g_i^o \\ 1 & \omega_k & \omega_k g_i^o g_j^o \end{vmatrix} \tag{C.14}$$

$$N_{ijk} = T_{ijk}^1 + T_{ijk}^2 + T_{ijk}^3 + T_{ijk}^4 \tag{C.15}$$

where

$$T_{ijk}^4 = \begin{vmatrix} 1 & \omega_i & \omega_i n_{jk} \\ 1 & \omega_j & \omega_j n_{ki} \\ 1 & \omega_k & \omega_k n_{ij} \end{vmatrix} . \tag{C.16}$$

We have now to demonstrate that the main cosmological operator G_{ijk}^{main} is equal to zero for the value of the actual cosmological parameters (Ω_o, λ_o) independently of the potential of the cluster (Actually, in the following lines we give a demonstration of Eq. (12)). To see that we can rewrite Eq. (C15) as

$$G_{ijk}^{main}(\Omega_o, \lambda_o) = \begin{vmatrix} 1 & \omega_i^o & \omega_i^o/g_i^o \\ 1 & \omega_j^o & \omega_j^o/g_j^o \\ 1 & \omega_k^o & \omega_k^o/g_k^o \end{vmatrix} g_i^o g_j^o g_k^o \, , \tag{C.17}$$

which is developed in (using Eq. (11))

$$g_i^o g_j^o g_k^o \left(\begin{vmatrix} 1 & \omega_i^o & 1 \\ 1 & \omega_j^o & 1 \\ 1 & \omega_k^o & 1 \end{vmatrix} \frac{1}{\gamma_\infty} + \begin{vmatrix} 1 & \omega_i^o & \omega_i^o \\ 1 & \omega_j^o & \omega_j^o \\ 1 & \omega_k^o & \omega_k^o \end{vmatrix} \frac{\kappa_\infty}{\gamma_\infty} \right) . \tag{C.18}$$

This demonstrates the zero value of $G_{ijk}^{main}(\Omega_o, \lambda_o)$ whatever the values of κ_∞ and $\boldsymbol{\gamma}_\infty$ are, *i.e* independently of the mass potential of the cluster.

Finally, let us now detail each term of the noise N_{ijk} and show their random behavior around zero, when considering different triplets (ijk). We first account for the behavior of T_{ijk}^4. It is built with terms like $\boldsymbol{p}_s^n$ ($n = 1$ to 3, $s = i, j$ or k) which all have simple properties:

- The real part of $\boldsymbol{p}_s^n$, $R_e(\boldsymbol{p}_s^n)$ has a random behavior centered on zero, for many triplets (i, j, k).
  In other words it means that the average of these terms behaves proportionally to the inverse of the square root of the number of triplets (or sources in the case of $\boldsymbol{p}^3$, because for a given galaxy taken in different triplets, the associated terms $\Delta\boldsymbol{\gamma}_\infty$ differ from each other, due to the random relative geometrical positions of galaxies in each triplet). The random position of galaxies in triplets implies that the term $\boldsymbol{p}^3$ has random orientation. This is also the case for $\boldsymbol{p}^1$ and $\boldsymbol{p}^2$ because the orientation of both the intrinsic source ellipticities and the ellipticity measurement errors are random. For the intrinsic source ellipticities, it is one of the postulates of the weak-lensing theory. For the ellipticity measurement errors, we see that this property will be true even if we consider small systematics due to the instrument point spread function (PSF) for example. Indeed, the orientation of the PSF is also random when taking in account different image positions around a cluster, a fortiori on many clusters.
- $R_e(\boldsymbol{p}_{s1}^n)$ and $R_e(\boldsymbol{p}_{s2}^n)$ are independent if $s1$ and $s2$ are two sources with different redshift.
  Once again this property comes from the random orientation of the $\boldsymbol{p}_s^n$ terms.

Both properties directly prove that the behavior of T^4 is random and centered on zero, since T^4 is made of a sum of terms proportional to $\boldsymbol{p}_s^n$ or $\boldsymbol{p}_{s1}^n \boldsymbol{p}_{s2}^{n*}$ (with $s1$ and $s2$ different. see Eqs. (C12), (C13) and (C17)).

We will now consider the quantities T^1, T^2 and T^3, which are made of terms like $\Delta\omega$. The probability distribution of these terms may not be exactly centered on zero. However, since we know the distributions of redshift and of errors on redshifts (shift between the photometric and the true redshifts), we can exactly correct the resulting bias. The principle is given in Sect. 4.1. It consists in recentring the $\Delta\omega$ distribution around zero. This is done by replacing each term ω by $\omega - \bar{\Delta\omega}$ (see Eq. (27)). In this case T^1 and T^2 are randomly distributed and are centered on zero, since they results from the addition of terms proportional to $\Delta\omega$. This applies also for T^3 which is made of terms proportional to $\Delta\omega_{s1}\Delta\omega_{s2}$ (with $s1 = i, j$ or k and $s2 = i, j$ or k different).

In conclusion the global behavior of the N_{ijk} terms is a random process centered on zero. Therefore, the GN term (which is the average of N_{ijk} on many triplets) decreases as the inverse of the square root of the number of sources.

References

Bonnet H., 1995, Ph.D. Thesis, Université Paul Sabatier, Toulouse, France

Brainerd T.G., Blandford R.D., Smail I., 1996, ApJ 466, 623

Breimer T.G., Sanders R.H., 1992, MNRAS 257, 97

Broadhurst T., 1998, In: Paul J., Montmerle T., Aubourg E. (eds.) Proceedings of the 19^{th} Texas symposium

Brunner R.J., Connoly A.J., Szalay A.S., Bershady M.A., 1997, ApJ 482, L21

Efstathiou G., Bridle S.L., Lasenby A.N., Hobson M.P., Ellis R.S., 1999, MNRAS 303, L47

Erben T., van Waerbeke L., Mellier Y., et al., 1999, astro-ph/9907134

Fort B., Mellier Y., Dantel-Fort M., 1996, A&A 321, 353

Helbig P., 1999, astro-ph/9904311

Hogg D.W., Cohen J.G., Blandford R., et al., 1998, AJ 115, 1418

Kovner I., 1987, ApJ 316, 52

Link R., Pierce M., 1998, ApJ 502, 63

Lombardi M., Bertin G., 1998, astro-ph/9806282

Mellier Y., 1998, ARA&A 37, in press astro-ph/9812172

Perlmutter S., Aldering G., Goldhaber G., et al., 1998, astro-ph/9812133

Schneider P., Rix H-W., 1996, ApJ 474, 25

Schneider P., Ehlers J., Falco E.E., 1992, Gravitational Lenses. Springer

Schneider P., 1996, MNRAS 283, 837

Seitz C., Schneider P., 1997, A&A 318, 687

Van Waerbeke L., Bernardeau F., Mellier Y., 1999, A&A 342, 15